Date Received: 04 Jan 2021

Effect of Environmental Factors on the Degradation of Organic Dyes by Electro-Fenton Using Carbon Felt Cathode

Nguyen Trung Dung[1]*, Le Thuy Duong[1], Nguyen Thi Hoa[1], and Nguyen Nhat Huy[2,3,*]

[1]Faculty of Physical and Chemical Engineering, Le Quy Don Technical University
236 Hoang Quoc Viet St., Bac Tu Liem District, Hanoi, Vietnam

[2]Faculty of Environment and Natural Resources
Ho Chi Minh City University of Technology (HCMUT)
268 Ly Thuong Kiet St., District 10, Ho Chi Minh City, Vietnam

[3]Vietnam National University Ho Chi Minh City
Linh Trung Ward, Thu Duc District, Ho Chi Minh City, Vietnam

Keywords: advanced oxidation process, carbon felt,
Electro-Fenton process, organic dyes, wastewater treatment

ABSTRACT

In this study, an electro-Fenton (EF) process using carbon felt (CF) as the cathode and titanium/platinum (Ti/Pt) as the anode was tested for removing ~~Rhodamine~~ rhodamine B (RhB) and other organic dyes in water. Characterization of the CF~~carbon felt~~ material was conducted by scanning electron microscopy (SEM) and X-ray powder diffraction (XRD). The influence of various environmental factors (*i.e.* solution pH, current density, catalyst dosage, RhB concentration, and type of dyes and electrolytes) on the dye removal was investigated. The results show that the maximum removal efficiency of RhB was 98% within 15 min at the optimal conditions of 50 mgRhB/L, 0.05 M Na_2SO_4, pH 3, 0.1 mM Fe^{2+}, and 6.67 mA/cm^2. The decomposition of RhB follows a pseudo-first-

*Corresponding Author: nguyentrungdung1980@gmail.com
nnhuy@hcmut.edu.vn

order model with the decomposition rate constant of 0.256 min^{-1}. Radical quenching experiments show that superoxide plays a key role in RhB degradation. Finally, results show that CFcarbon felt has high stability and degradation efficiency, which is suitable as a cathode for the removal of organic dyes in wastewater.

INTRODUCTION

Textile wastewater is one of the most popular types of industrial wastewater in developing countries such as Vietnam, which is characterized by high color, COD, BOD, and soluble dyes. Among the dyes, Rhodamine B (RhB) is an essential cationic xanthene dye (Figure 1), which is fast color, inexpensive, and widely used in the industry. Since RhB and other dyes are toxic and hazardous (Nidheesh *et al.* 2014), the removal of these dyes is necessary before discharging them into the water environments. There are many techniques to remove RhBRhodamine B in water, such as adsorption (Wu *et al.* 2020; Xiao *et al.* 2020), membrane separation (Saja *et al.* 2020; Sundaran *et al.* 2019), and advanced oxidation processes (AOPs) – including catalytic activation (Pang *et al.* 2019; Zhu *et al.* 2019), photocatalysis (Yang *et al.* 2020; Zhang *et al.* 2020a), Fenton (Hou *et al.* 2011), photo-Fenton (Gao *et al.* 2015), UV/EFelectro-Fenton (Zhang *et al.* 2020b), and EFelectro-Fenton (Yuan *et al.* 2011; Ai *et al.* 2008; Nidheesh and Gandhimathi 2014a, b; Nidheesh *et al.* 2014; Nidheesh and Gandhimathi 2014a; Tian *et al.* 2016). Among them, electro-Fenton (the EF) process is one of the most effective methods for the fast degradation of persistent organic pollutants. Since EF is one of the Fenton processes, it still has some similar limitations to the traditional Fenton process, such as low working pH, consumption of acid for reaction and alkali for neutralization, as well as the

Formatted: Highlight

*Corresponding Author: nguyentrungdung1980@gmail.com
nnhuy@hcmut.edu.vn

Date Received: 04 Jan 2021

requirement of electricity use. However, the EF process has many advantages such as high flexibility, ~~easy~~ ease ~~t~~of control, automation, high efficiency, and environmental compatibility. Moreover, the EF process is also better than the conventional Fenton process in terms of ~~(i)~~ the *in -situ* H_2O_2 production and ~~(ii) the~~ continuous Fe^{2+} regeneration, which provides an easy chemical operation, improves the oxidation process, and reduces the sludge production.

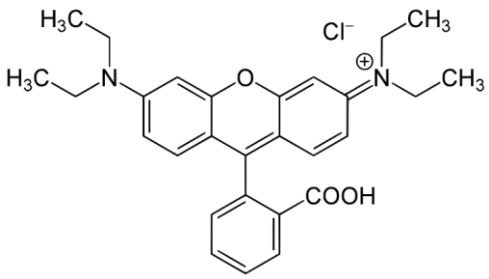

Figure 1. Structure of RhB~~rhodamine B~~.

The principle of the EF process is similar to that of the conventional Fenton process, which is the generation of hydroxyl radicals (•OH, Reaction 1) and its consumption by the organics (Reaction 2). Here, Fe^{2+} is externally added and regenerated by electrochemical reduction (Reaction 3), while H_2O_2 is on-site supplied from the cathode by the reduction of oxygen in water (Reaction 4). H_2O_2 can also be decomposed into H_2O and O_2 at high solution pH values (Reaction 5) or reacts with •OH (Reaction 6). The •OH can also be consumed by Fe^{2+} under a high concentration of Fe^{2+} but a low concentration of reductants (*e.g.* organics) (Reaction 7).

$$H_2O_2 + Fe^{2+} \rightarrow Fe^{3+} + OH^- + {}^{\bullet}OH \quad (1)$$

*Corresponding Author: nguyentrungdung1980@gmail.com
nnhuy@hcmut.edu.vn

Formatted: Font: Italic
Formatted: Highlight
Formatted: Highlight
Formatted: Highlight
Formatted: Highlight
Formatted: Highlight
Formatted: Highlight
Formatted: Highlight
Formatted: Highlight
Formatted: Highlight

$RH + {}^{\bullet}OH \rightarrow R^{\bullet} + H_2O$ (2)

$Fe^{3+} + e \rightarrow Fe^{2+}$ (3)

$O_2 + 2H^+ + 2e \rightarrow H_2O_2$ (4)

$2H_2O_2 \rightarrow 2H_2O + O_2$ (5)

$2{}^{\bullet}OH + H_2O_2 \rightarrow 2H_2O + O_2$ (6)

$Fe^{2+} + {}^{\bullet}OH \rightarrow Fe^{3+} + OH^-$ (7)

Several ~~electro-Fenton~~EF parameters affect its efficiency for water treatment, such as electrode material, catalyst concentration, current density, and solution pH. Among them, the cathode material is important because it determines the H_2O_2 production and, therefore, affects the •OH generation rate (Reaction 1). Carbonaceous materials are commonly used as cathodes, including carbon foam, CF~~carbon felt~~, boron-doped diamond, graphite, and graphite felt. With good stability, high conductivity, high surface area, abundant resources, and low cost, ~~carbon felt (~~CF~~)~~ is a good candidate for use as cathode material in electrochemistry (Huong Le *et al.* 2017; Mi *et al.* 2019). There have been several reports of using CF as a cathode for EF~~electro-Fenton~~. In the work of Pimentel *et al.* (2008), the EF process could remove 100% of total organic carbon (TOC) in phenol treatment under optimum conditions of 10^{-4} M of $FeSO_4$. Sirés *et al.* (2007) also using CF as cathode for EF treatment of antimicrobial triclosan and triclocarban. Dyes such as triphenylmethane (*e.g.* malachite green, crystal violet, methyl green, and fast green FCF) and azo (*e.g.* azobenzene, p-methyl red, and methyl orange) were effectively treated by EF process using CF cathode (Sirés *et al.* 2008; Guivarch *et al.* 2003). Moreover, the pesticide (Zazou *et al.* 2016; Tran *et al.* 2019) and antibiotics (Wu *et al.* 2012; El-Ghenymy *et al.* 2014) in water was also efficiently removed and mineralized by

*Corresponding Author: nguyentrungdung1980@gmail.com
nnhuy@hcmut.edu.vn

EF treatment using CF cathode. However, there is very limited information on the application of CF~~carbon felt~~ as cathode for removal of RhB~~Rhodamine B~~ in water and on the effect of environmental factors on the efficiency of the EF~~electro-Fenton~~ process.

In this work, we used commercially available CF~~carbon felt~~ as a cathode electrode for the EF process and tested its performance for the removal of RhB as well as other dyes in water. The effects of environmental factors such as solution pH, applied current density, Fe^{2+} concentration, and RhB concentration were investigated. The role of electrolytes and reactive oxidation species were also determined.

MATERIALS AND METHODS

All chemicals used in this study are pure chemicals with a purity of ≥ 99%. Chemicals such as ~~Rhodamine B (~~RhB~~)~~, ~~Tartrazine~~ tartrazine (TTZ), Janus ~~Green~~ green B (JGB), ~~Direct~~ direct ~~Blue~~ blue 71 (DB71), ~~Methylene~~ methylene ~~Blue~~ blue (MB), p-benzoquinone (p-BQ), furfuryl alcohol (FFA), and tert-butanol alcohol (TBA) were purchased from Shanghai Macklin (China). Other chemicals such as $FeSO_4.7H_2O$, Na_2SO_4, NaCl, $NaNO_3$, H_2SO_4, and NaOH were obtained from Xilong (China). CF~~Carbon felt~~ was supplied by Hebei Xingshi (China). Double-distilled water was taken locally from the lab.

The morphology of the CF~~carbon felt~~ was determined by ~~scanning electron microscopy~~SEM (~~SEM,~~ Hitachi S-4800, Japan)~~.~~. The ~~X-ray powder diffraction (~~XRD~~)~~ pattern was collected by a Bruker D8 Advance X-ray diffractometer with Cu Ka radiation

*Corresponding Author: nguyentrungdung1980@gmail.com
nnhuy@hcmut.edu.vn

Date Received: 04 Jan 2021

(λ = 1.5406 Å) with a step scan of 0.02° and step time of 1 s. The absorbance of the solution was measured by a UV-Vis spectrophotometer (Biochrom SP-60, UK).

The experiments for EF~~electro-Fenton~~ degradation of RhB were conducted at room conditions in a 500 mL glass beaker (Figure 2). In the reactor, CF~~carbon felt~~ with a dimension of 12 cm × 5 cm was used as cathode and Pt/Ti material was used as an anode. The anode and cathode were placed parallel and the distance between them was set at 3 cm in all the experiments. Electrolyte (50 mM Na_2SO_4) was added into the dye (50 mg/L RhB) solution and stirred vigorously and the solution pH was adjusted to 3 by using sulfuric acid. The solution was aerated 15 min before and kept aeration during the experiment. $FeSO_4$ (0.1 mM) was used as a Fenton catalyst and a constant DC current of 400 mA (BC 1830, LiOA, Vietnam) was used as a current supply. All the experiments were repeated ~~3~~ three times and the average results, as well as their standard deviations, were reported.

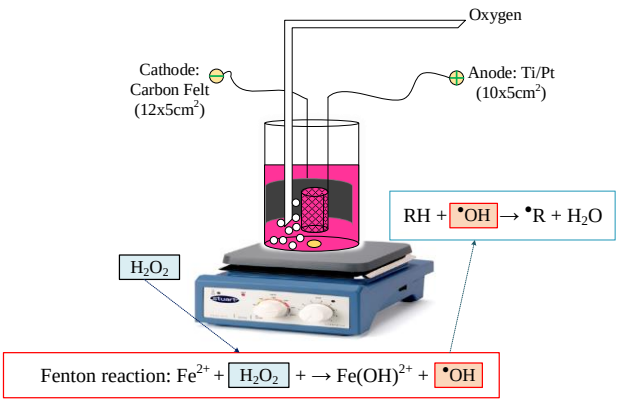

Figure 2. Schematic presentation of the EF~~electro-Fenton~~ system.

*Corresponding Author: nguyentrungdung1980@gmail.com
nnhuy@hcmut.edu.vn

During the reaction, water samples with a volume of 4 mL were taken, centrifuged, and sent for absorbance measurement at 554 nm to determine the RhB concentration. In this study, the EF process was also applied for other dyes in different types of xanthene (*e.g.* RhB), azo (*e.g.* TTZ, DB71, and JGB) and thiazine (*e.g.* MB) to evaluate the possibility of the EF process for treatment of various types of dyes in practical applications. The experiments for other dyes were conducted under the same condition of RhB~~Rhodamine B~~ and the concentrations of the dyes were measured at wavelengths of 428, 587, 654, and 664 nm for TTZ, DB71, JGB, and MB, respectively. The calculation for removal efficiency and the fitting of the pseudo-first-order kinetic model for the removal of RhB are as follows (Afanga *et al.* 2021):

$$H(\%) = (1 - C_t/C_o) \times 100 \quad (8)$$

$$\ln(C_t/C_0) = k_{app} \times t \quad (9)$$

where C_o and C_t (mg/L) are the concentration of RhB at the beginning and after the reaction, respectively, and k_{app} (min^{-1}) is the rate constant for the pseudo-first-order kinetic model.

To investigate the key reactive oxygen species involved in RhB degradation, three scavengers (*i.e.* 50 mM TBA, 1 mM p-BQ, and 50 mM FFA) were added to quench hydroxyl radical ($k_{TBA\text{-}HO\bullet}$ = 3.8–7.6 × 10^8 M^{-1} s^{-1}), superoxide radical ($k_{pBQ\text{-}O2\bullet-}$ = 9.8 × 10^8 M^{-1} s^{-1}), and singlet oxygen ($k_{FFA\text{-}^1O2}$ = 1.2 × 10^8 M^{-1} s^{-1}) (Yu *et al.* 2020; Chen *et al.* 2020), respectively, before turning on the electricity for EF process.

Formatted: Highlight

Formatted: Highlight

Formatted: Highlight

*Corresponding Author: nguyentrungdung1980@gmail.com
nnhuy@hcmut.edu.vn

The recyclability of the electrodes was also conducted *via* ~~5~~ five cycles of RhB treatment by the EF process. After each experiment, the used CF~~carbon felt~~ electrode was washed thoroughly with distilled water and ethanol to remove the organics. After that, the electrodes were dried at 80 °C in an oven and then reused for the next cycle of RhB removal by the EF process.

RESULTS AND DISCUSSION

Characteristics of the ~~Carbon Felt~~CF Cathode

As shown in Figure ~~3(a)~~, the commercial CFs are fine fibers with a diameter of about 20 μm. They have a clean and smooth surface, which is free of adhered organic and inorganic impurities. The fibers are randomly dispersed with a relatively homogeneous space between them. The XRD pattern of CF is displayed in Figure 3~~(b)~~. There are two weak peaks observed at 2θ of around 25° and 43°, which correspond to the (002) and (100) crystal planes of the CF material. These results also indicate the amorphous structure of CF, which is consistent with previous work (Ganiyu *et al.* 2017; Huong Le *et al.* 2017).

Formatted: Highlight

Formatted: Highlight

Formatted: Highlight

Formatted: Highlight

*Corresponding Author: nguyentrungdung1980@gmail.com
nnhuy@hcmut.edu.vn

Date Received: 04 Jan 2021

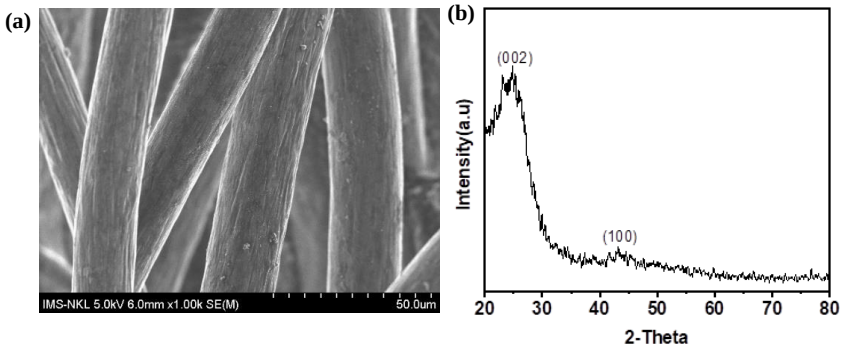

Figure 3. (a) SEM images and (b) XRD pattern of the CF~~carbon felt~~ cathode.

Formatted: Highlight

Degradation of Rh~~odamine~~ B by EF Process Using CF Cathode

The effect of pH on the performance of the EF process for RhB removal was investigated in the initial pH range of 2.0, 2.5, 3.0, 3.5, and 4.0. As seen in Figure 4~~(~~a~~)~~, high RhB removal efficiencies of around 98% were observed in a narrow pH range from 2.0 ~~to~~ 3.5 after 15 min of treatment, while the efficiency was only at 3.2% for pH 4.0. The acidic conditions favor the formation of H_2O_2 at the cathode. Also, the hydroxyl radical has stronger oxidation properties under acidic conditions than under neutral or basic conditions. When pH ≥ 4, H_2O_2 was preferentially broken down into O_2 and H_2O (Reaction 5), while Fe^{2+} and Fe^{3+} forms iron hydroxide complexes, thus reducing the Fe(III) catalyst in the solution and lose its activity. These lead to a decrease in the formation of reactive oxygen species and, therefore, the RhB degradation efficiency (Lin *et al.* 2014; Nidheesh *et al.* 2014) since the main removal mechanism is *via* coagulation or adsorption. Although pH 2 shows slightly better removal efficiency than pH 3, running the EF process at pH 2 consumes a sustainably higher amount of acid than that at pH 3 and requires much more

Formatted: Highlight

Formatted: Highlight

Formatted: Highlight

Formatted: Highlight

Formatted: Highlight

*Corresponding Author: nguyentrungdung1980@gmail.com
nnhuy@hcmut.edu.vn

alkali solution for neutralization after treatment. Also, a very low pH of 2 could easily cause corrosion issues for the equipment in water treatment. Therefore, pH 3 was chosen as a suitable pH for further EF~~electro-Fenton~~ experiments. The pH change according to the degradation time of RhB was also investigated. The results in Figure 4~~(~~b~~)~~ show that there was a slight pH increase during the first 3 min of reaction, which may be due to the production of OH^- by EF process. After that, there was a slight decrease in pH value, which could be due to the formation of short-chain carboxylic acids during the EF process (Nidheesh *et al.* 2014; Gao *et al.* 2015). Generally, it can be considered that the solution pH value is relatively stable during the EF process.

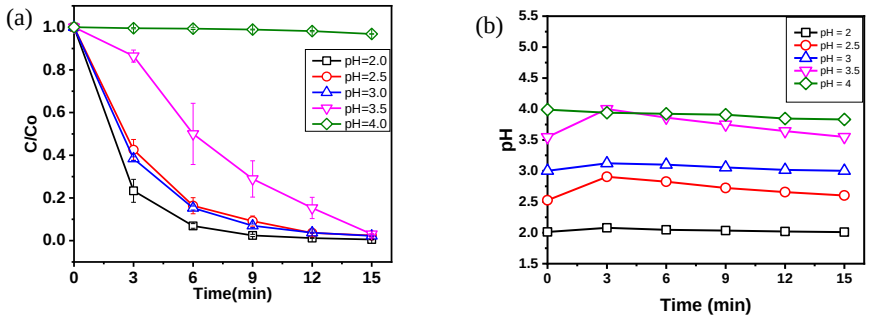

Figure 4. (a) Effect of initial solution pH on the EF removal of RhB and (b) pH change with time during the EF process. Experimental conditions: 50 mgRhB/L, 0.1 mM Fe^{2+}, 6.67 mA/cm^2, 50 mM Na_2SO_4.

The applied current density affects the formation rate of both H_2O_2 (Reaction 4) and $^{\bullet}OH$ (Reaction 1). The experiments were conducted in the current density range from 1.67~~ to~~ 8.33 mA/cm^2 (Figure 5~~(~~a~~)~~). The degradation of RhB well fitted with the first-order

*Corresponding Author: nguyentrungdung1980@gmail.com
nnhuy@hcmut.edu.vn

Date Received: 04 Jan 2021

kinetics equation (Figure 5(b)) with $R^2 \geq 0.98$. The degradation rate constant of RhB increased by 3 three times (*i.e.* from 0.08324 to 0.255 min^{-1}) when the current density increased from 1.67 to 6.67 mA/cm^2. After 15 min of the experiment (Figure 5(a)), the RhB removal efficiencies were 76.57, 92.21, 96.51, 97.77, and 94.80% at 1.67, 3.33, 5.00, 6.67, and 8.33 mA/cm^{-2}, respectively, indicating a proportional relationship of RhB degradation and current density in the range of 1.67 to 6.67 mA/cm^2. This is due to an increase in the electrochemical formation of H_2O_2 (Reaction 4), which increases the conversion of Fe^{3+} to Fe^{2+} with the increased current density (Annabi *et al.* 2016). Since RhB is a cationic dye, it is more attracted towards the cathode under higher current density. This increases the frequency of collisions between dyes molecule and reactive oxygen species, thus improves the RhB removal in water. However, as the applied current density continued to increase to 8.33 mA/cm^2, the RhB decomposition efficiency decreased. The cause may be due to the degradation reactions of H_2O_2 and other reactive oxygen species (Reactions 5 and 6) at high current density (Lin *et al.* 2017), resulting in a reduced rate of RhB decomposition. Therefore, the current density of 6.67 mA/cm^2 was selected for the next experiments.

Formatted: Highlight
Formatted: Highlight
Formatted: Highlight
Formatted: Highlight
Formatted: Highlight
Formatted: Highlight
Formatted: Highlight
Formatted: Highlight

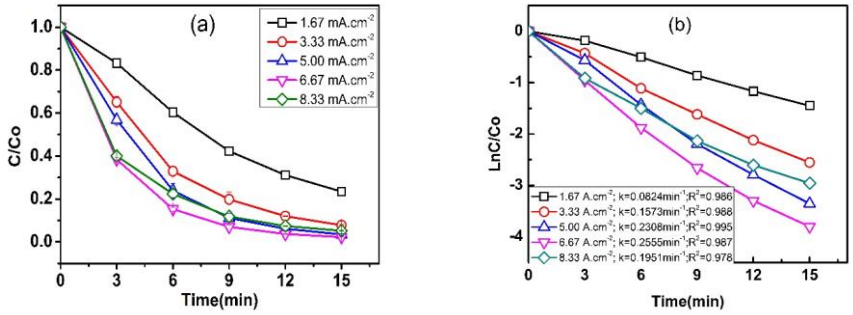

*Corresponding Author: nguyentrungdung1980@gmail.com
nnhuy@hcmut.edu.vn

Figure 5. (a) Influence of applied current density on RhB degradation and (b) the degradation kinetics for the pseudo-first-order reaction of RhB. Experimental conditions: 50 mgRhB/L, 0.1 mM Fe^{2+}, pH 3.0, 50 mM Na_2SO_4.

The concentration of Fe^{2+} is an important factor that affects the RhB removal, which is presented in Figure 6. One can see that the rate of RhB removal increases when the Fe^{2+} concentration increase from 0.025 mM to 0.1 mM and then decreases with a further increase of Fe^{2+} concentration. The decreased rate of RhB at a high concentration of Fe^{2+} catalyst (> 0.1 mM) is attributed to the role of Fe^{2+} as a scavenger of $^{\bullet}OH$ (Reaction 7) with a high rate constant of $k = 3.20 \times 10^8$ $M^{-1}s^{-1}$. Therefore, 0.1 mM was chosen as a suitable Fe^{2+} concentration for the following experiments.

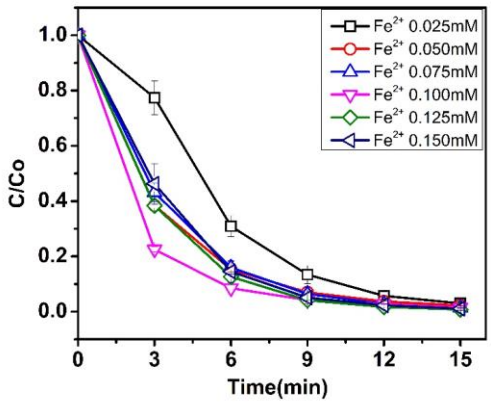

Figure 6. Effect of Fe^{2+}) concentration on RhB degradation. Experimental conditions: 50 mgRhB /L, pH 3.0, 6.67 mA/cm^2, 50 mM Na_2SO_4.

*Corresponding Author: nguyentrungdung1980@gmail.com
nnhuy@hcmut.edu.vn

Figure 7 shows a decrease in RhB removal efficiency with the increasing initial RhB concentration. When the concentration increased from 25 to 50, 75, and 100 mg/L, the removal efficiency after 15 min of reaction decreased from 100 to 97.77, 95.64, and 90.91% respectively. This is due to the deficiency of reactive oxygen species for the removal of RhB under high concentrations.

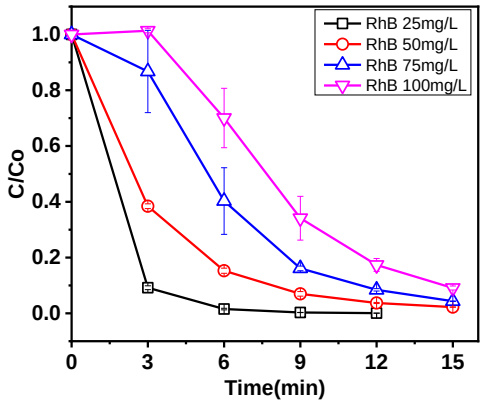

Figure 7. Influence of initial RhB concentration on its degradation. Experimental conditions: pH 3.0, 0.1 mM Fe^{2+}, 6.67 mA/cm^2, 50 mM Na_2SO_4.

UV–Vis spectra of RhB in the solution during the degradation time are plotted in Figure 8. The characteristic absorption peak is observed at 554 nm. The peak at 517 nm is attributed to the n-π* transitions of C=N and C=O groups while the peak at 352 nm is ascribed to the naphthalene ring bonded to the –C=N– group. The shoulder peaks (*i.e.* at 283 and 307 nm) of 257 nm peak corresponds to the π-π* transition associated with aromatic rings. The decline of the characteristic peak demonstrates the rapid degradation

*Corresponding Author: nguyentrungdung1980@gmail.com
nnhuy@hcmut.edu.vn

Formatted: Highlight
Formatted: Highlight
Formatted: Highlight

231 of RhB in the first 3 min. The disappearance of the adsorption band during reaction time
232 indicates the degradation in the structure of RhB molecules by the reactive oxygen
233 species produced during the EF process.

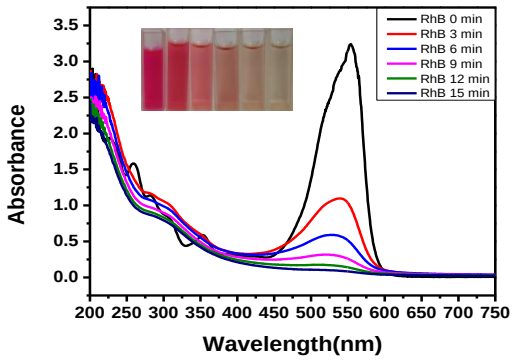

234

235 **Figure 8.** UV-Vis spectra of RhB at different degradation times. Experimental
236 conditions: 50 mg RhB/L, pH 3.0, 0.1 mM Fe^{2+}, 6.67 mA/cm^2, 50 mM Na_2SO_4.

237 To determine the applicability of the EF process in practical wastewater, the
238 optimal condition of the EF process was applied for the decomposition of different groups
239 of dyes such as azo dyes (*i.e.* TTZ, DB71, and JGB), phenothiazine (*i.e.* MB), and
240 xanthene (*i.e.* RhB). Figure 9 shows a decreasing order of decomposition efficiency as
241 RhB (98%) ≈ TTZ (97%) > JGB (80%) ≈ DB71 (79%) > MB (70%). The difference in the
242 degradation efficiency of dyes can be attributed to the difference in their structures. The
243 easy dissociation of π-bondings (*e.g.* to form naphthalene ring) of TTZ, DB71, and JGB
244 (with –N=N– color centers) make them easier to be degraded (Oancea and Meltzer 2013;
245 Maleki *et al.* 2015). Regarding thiazine dye (MB), aromatic ring-bonded nitrogen atoms

Formatted: Highlight
Formatted: Highlight
Formatted: Highlight
Formatted: Highlight

*Corresponding Author: nguyentrungdung1980@gmail.com
nnhuy@hcmut.edu.vn

were first degraded due to their electron-donating groups [(–N(CH$_3$)$_2$)] (Teng *et al.* 2020). On the other hand, the decomposition of conjugated structure and subsequent N-demethylation in xanthene dye (RhB) is its main degradation mechanism (Gazi *et al.* 2010). The results indicated that the EF process using CF carbon felt could be widely used to degrade different dyes.

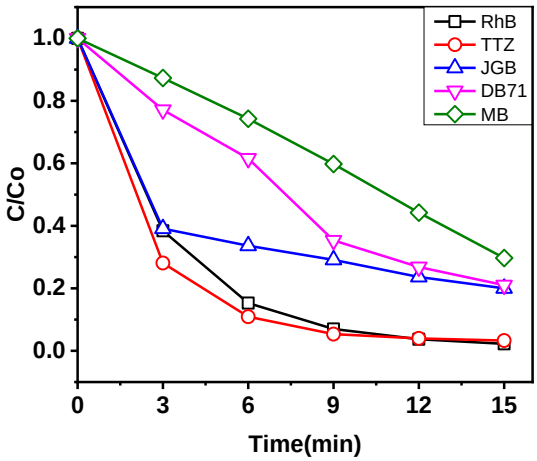

Figure 9. The degradation of different dyes by the EF process. Experimental conditions: 50 mg dye/L, pH 3.0, 0.1 mM Fe^{2+}, 6.67 mA/cm^2, 50 mM Na_2SO_4.

To find the effect of electrolyte types on the RhB degradation, 50 mM of sodium salts (*i.e.* chloride, nitrate, and sulfate) were added to the EF system. As seen in Figure 10, a complete removal of RhB can be observed within 15 min in the presence of Na_2SO_4 and NaCl. When using Na_2SO_4 as an electrolyte, sulfate radicals ($SO_4^{\bullet-}$) (E^o = 2.6 – 3.2 V) are formed at the anode surface from the Reactions (10 – 12), which could contribute

*Corresponding Author: nguyentrungdung1980@gmail.com
nnhuy@hcmut.edu.vn

to the decomposition of RhB~~Rhodamine B~~. Sulfate radical has a long existence time in the solution and has a strong redox ability, which facilitates the selective oxidation of organic pollutants in water (Hai *et al.* 2020).

$$2SO_4^{2-} \rightarrow S_2O_8^{2-} + 2e \quad (8)$$

$$S_2O_8^{2-} + e \rightarrow SO_4^{\bullet-} + SO_4^{2-} \quad (9)$$

$$2SO_4^{2-} + HO^{\bullet} \rightarrow SO_4^{\bullet-} + HO^{-} \quad (10)$$

In the case of NaCl, active chlorine forms (*e.g.* Cl_2, HClO, ClO^-, and Cl•) are formed in solution by the direct oxidation of the chloride anion at the anode surface, which also enhances the degradation of RhB. However, these chlorine forms can also react with organics to form chlorinated organics, which are hazardous compounds.

$$2Cl^- \rightarrow Cl_2 + 2e \quad (13)$$

$$Cl_2 + H_2O \rightarrow HClO + HCl \quad (14)$$

$$2Cl^- + HO^{\bullet} \rightarrow Cl^{\bullet} + HO^- \quad (15)$$

$$Cl^{\bullet} + Cl^{\bullet} \rightarrow Cl_2 \quad (16)$$

However, with $NaNO_3$, there was complete inhibition of RhB degradation. This can be explained that nitrate ions and nitrite are reduced at the cathode to form ammonia, which can react with hydroxyl radicals, leading to the inhibition of RhB degradation. The degradation rate constant (k_{app}) of RhB using $NaNO_3$ was 0.0022 min^{-1}, which was 110 and 120 times lower than those using NaCl and Na_2SO_4, respectively.

$$NO_3^- + 6H_2O + 8e \rightarrow NH_3 + 9HO^- \quad (17)$$

$$NO_3^- + 2H^+ + 2e \rightarrow NO_2^- + H_2O \quad (18)$$

*Corresponding Author: nguyentrungdung1980@gmail.com
nnhuy@hcmut.edu.vn

Formatted: Highlight
Formatted: Pattern: Clear (Green)
Formatted: Highlight
Formatted: Not Highlight
Formatted: Not Highlight

Date Received: 04 Jan 2021

$NO_2^- + 5H_2O + 6e \rightarrow NH_3 + 7HO^-$ (19~~7~~)

$2NH_3 + 6HO^\bullet \rightarrow N_2 + 6H_2O$ (2018)

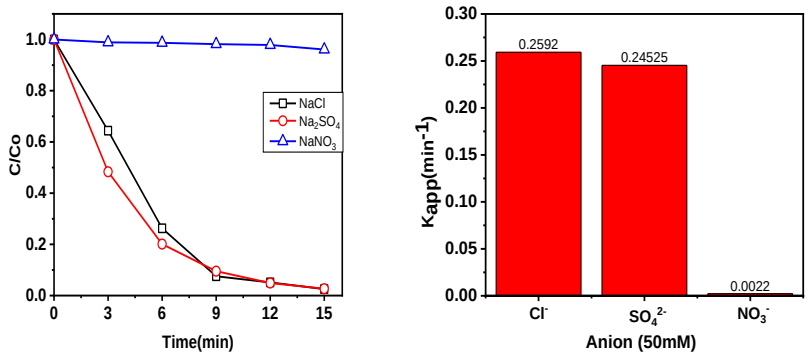

Figure 10. (a) Effects of electrolyte on RhB degradation and (b) the degradation rate constant. Experimental conditions: 50 mg RhB/L, pH 3.0, 0.1 mM Fe^{2+}, 6.67 mA/cm^2, 50 mM of electrolyte.

As illustrated in Figure~~,~~ 11, the RhB degradation efficiency decreased from 98% to 85~~%~~, 81~~%~~, and 36% when using TBA, FFA, and p-BQ, respectively. Therefore, the role of the reactive species is in the other of $O_2^{\bullet-}$ > $^1O_2$ ≈ $HO^\bullet$, proving the role of oxygen in the formation of reactive oxygen species. When replacing air with pure nitrogen gas, the degradation efficiency decreased from 98~~%~~ to 68%. Thus, oxygen plays an important role in forming active oxygen species (*e.g.* $O_2^{\bullet-}$, $^1O_2$, and $HO^\bullet$), which determine the degradation efficiency of RhB.

*Corresponding Author: nguyentrungdung1980@gmail.com
nnhuy@hcmut.edu.vn

Date Received: 04 Jan 2021

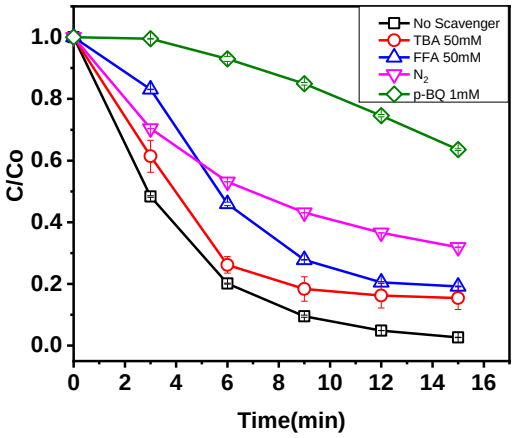

Figure 11. RhB degradation in the presence of different radical scavengers. Experimental conditions: 50 mgRhB/L, pH 3.0, 0.1 mM Fe^{2+}, 6.67 mA/cm^2, 50 mM Na_2SO_4, 50 mM of scavenger.

The stability of the cathode electrode is an essential issue for practical applications. As seen in Figure 12, it is interesting that there was no apparent decrease in the RhB degradation efficiency during ~~5~~ five cycles of RhB treatment by EF process, indicating that the CF~~carbon felt~~ is very stable and reusable, which is a very potential electrode for practical wastewater treatment using the EF~~electro-Fenton~~ system.

Formatted: Highlight

Formatted: Highlight

*Corresponding Author: nguyentrungdung1980@gmail.com
nnhuy@hcmut.edu.vn

Date Received: 04 Jan 2021

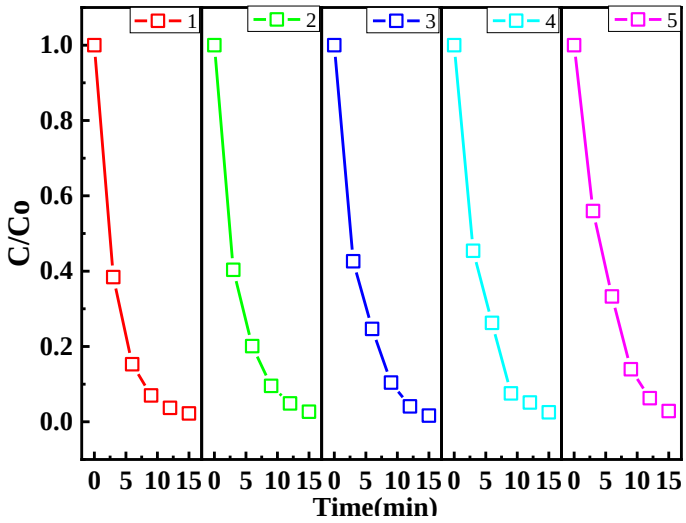

Figure 12. RhB degradation using recycled CF~~carbon felt~~ as cathode.

Table 1 summarizes the main results using CF~~carbon felt~~ as a cathode electrode in the EF process to remove various organic pollutants such as dyes, antibiotics, and pesticides. In most cases, the complete degradation of organic pollutants is considered to be the oxidation role of $HO^{\bullet}$. However, our research proved that RhB decomposition involves different types of active oxygen, in which superoxide radical plays a decisive role.

Table 1. Removal of organic pollutants by EF process using CF~~carbon felt~~ as the cathode electrode.

Formatted: Highlight

Formatted: Highlight

Formatted: Highlight

*Corresponding Author: nguyentrungdung1980@gmail.com
nnhuy@hcmut.edu.vn

Cathode electrode	Organic pollutants	EF conditions	Efficiency	Reference
~~Carbon felt~~CF (12 cm × 5 cm)	Rh~~odamine~~ B (RhB, $C_{28}H_{31}ClN_2O_3$)	[RhB] = 50 mg/L pH = 3.0 [Fe(II)] = 0.1 mM [Na_2SO_4] = 50 mM Anode: Ti/Pt (10 cm × 5 cm); Applied current density: 6.67 mA.cm^{-2}	Degradation of 98% RhB in 15 min of electrolysis Oxidation rate constant: 0.255 min^{-1} Order of reactive oxygen species: $O_2^{\bullet-}$ > $^1O_2$ ≈ HO$^\bullet$	Present study
~~Carbon felt~~CF (16 cm × 7 cm)	Orange II ($C_{16}H_{11}N_2NaO_4S$)	[Orange II] = 50 mg/L pH = 3.0 [Fe(III)] = 0.2 mM Anode: RuO_2-IrO_2 [Na_2SO_4] = 50 mM Applied current density: 1.78 mA.cm^{-2}	Degradation of 97.8% Orange II in 10 min of electrolysis HO$^\bullet$ played an important role in the oxidation process.	Lin *et al.* (2014)
~~Carbon felt~~CF (10 cm × 5 cm)	Glyphosate (Gly, $C_3H_8NO_5P$)	[Gly] = 0.1 M pH = 3	Degradation of 91.91% Gly in 40 min of electrolysis	Tran *et al.* (2019)

*Corresponding Author: nguyentrungdung1980@gmail.com
nnhuy@hcmut.edu.vn

Formatted: Highlight

Formatted: Highlight

		Anode: Pt (8 cm × 4 cm) Applied current density: 10 mA.cm^{-2}	Oxidation rate constant: 0.063 min^{-1} HO• played an important role in the oxidation process.	
~~Carbon Felt~~CF (8 cm × 6 cm)	Benzoic acid ($C_7H_6O_2$)	[Benzoic acid] = 0.2 mM pH = 3 [Fe(II)] = 0.3 mM Anode: BDD (8 cm × 5 cm) Applied current density: 6.25 mA.cm^{-2}	Degradation of 89% Benzoic acid in 60 min and 95% in 120 min of electrolysis	Sennaoui *et al.* (2019)
~~Carbon felt~~CF (15 cm × 4 cm)	Paraaminosalicylic acid (PAS, $C_7H_7NO_3$)	[PAS] = 0.1 mM (15.3 mg/L) pH = 3 [Fe(II)] = 0.1 mM [Na_2SO_4] = 50 mM Applied current density: 8.33 mA.cm^{-2} Anode: Pt and BDD	Degradation of 100% PAS in 7 min of electrolysis using Pt/carbon-felt cell and in 10 min using BDD/carbon-felt cell Oxidation rate constant: 4.17 × 10^9 M^{-1} s^{-1}	Oturan *et al.* (2018)

Formatted: Highlight

Formatted: Highlight

*Corresponding Author: nguyentrungdung1980@gmail.com
nnhuy@hcmut.edu.vn

			HO• played an important role in the oxidation process.	
~~Carbon Felt~~CF (17.5 cm × 6 cm)	Sucralose (SUS, $C_{12}H_{19}Cl_3O_8$)	[SUC] = 80 mg/L pH = 3 [Fe(II)] = 0.2 mM [Na_2SO_4] = 50 mM Anode: BDD (25 cm^2) Applied current density: 1.9 $mA.cm^{-2}$	Remove 96.1 % TOC of SUC in 120 min of electrolysis HO• played an important role in the oxidation process.	Lin *et al.* (2017)
~~Carbon felt~~CF (70 cm^2)	Enoxacin (ENXN, $C_{15}H_{17}FN_4O_3$)	[ENXN] = 50mg/L pH = 3 [Fe(II)] = 0.2 mM [Na_2SO_4] = 50 mM Anode: BDD (5 cm × 4 cm) Applied current density: 4.286 $mA.cm^{-2}$	Degradation of 98% ENXN in 60 min of electrolysis HO• played an important role in the oxidation process.	Annabi *et al.* (2016)
~~Carbon felt~~CF (14 cm × 5 cm)	Norfloxacin (Nor, $C_{16}H_{18}FN_3O_3$)	[Nor] = 0.25 mM pH = 3 [Fe(III)] = 0.1 mM	Remove 98 % TOC of Nor in 5 h of electrolysis	Özcan *et al.* (2016)

Formatted: Highlight

Formatted: Highlight

Formatted: Highlight

*Corresponding Author: nguyentrungdung1980@gmail.com
nnhuy@hcmut.edu.vn

		Anode: Pt and BDD (5 cm × 4 cm) Applied current density: 4.286 mA.cm^{-2}		
~~Carbon felt~~CF (60 cm^2)	Levofloxacin (Levo, $C_{18}H_{20}FN_3O_4$)	[Levo] = 83.6 mg/L pH = 3 [Fe(II)] = 0.2 mM Anode: BDD (6 cm^2) Applied current density: 5 mA.cm^{-2}	Remove 85 % TOC of Levo in 8 h of electrolysis HO• played an important role in the oxidation process.	Barhoumi *et al.* (2015)
~~Carbon felt~~CF (20 cm × 4 cm)	Tetracycline (TC, $C_{22}H_{24}N_2O_8$)	[TC] = 80 mg/L pH = 3 [Fe(II)] = 0.1 mM [Na_2SO_4] = 50 mM Anode: Ti/RuO_2-IrO_2 (36 cm^2) Applied current density: 5 mA.cm^{-2}	Remove 83.9 % TOC of TC in 8 h of electrolysis HO• played an important role in the oxidation process.	Chen *et al.* (2019)

Formatted: Highlight

Formatted: Highlight

CONCLUSIONS

*Corresponding Author: nguyentrungdung1980@gmail.com
nnhuy@hcmut.edu.vn

A comprehensive study was conducted to investigate the effect of environmental factors on the removal of RhB *via* the EF~~electro-Fenton~~ process using CF~~carbon felt~~ as the cathode material. The suitable condition was determined at RhB concentration of 50 mg/L, pH 3.0, Fe^{2+} concentration of 0.1 mM, current density of 6.67 mA/cm^2, and electrolyte of 50 mM Na_2SO_4. The effect of radical scavenger was also conducted, showing a decisive role of superoxide radical. The durability of the CF~~carbon felt~~ cathode was also tested by cycle test, which proves its stability for practical applications in wastewater treatment.

REFERENCES

AFANGA H, ZAZOU H, TITCHOU FE, GAAYDA JE, SOPAJ F, AKBOUR RA, HAMDANI M. 2021. Electrochemical oxidation of Naphthol Blue Black with different supporting electrolytes using a BDD /carbon felt cell. J Environ Chem Eng 9(1): 104498.

AI Z, XIAO H, MEI T, LIU J, ZHANG L, DENG K, QIU J. 2008. Electro-Fenton Degradation of Rhodamine B Based on a Composite Cathode of Cu_2O Nanocubes and Carbon Nanotubes. J Phys Chem C 112(31): 11929–11935.

ANNABI C, FOURCADE F, SOUTREL I, GENESTE F, FLONER D, BELLAKHAL N, AMRANE A. 2016. Degradation of enoxacin antibiotic by the electro-Fenton process: optimization, biodegradability improvement and degradation mechanism. J Environ Manage 165: 96–105.

Formatted: Highlight
Formatted: Highlight
Formatted: Highlight
Formatted: Highlight
Formatted: Highlight
Formatted: Highlight

*Corresponding Author: nguyentrungdung1980@gmail.com
nnhuy@hcmut.edu.vn

BARHOUMI N, LABIADH L, OTURAN MA, OTURAN N, GADRI A, AMMAR S, BRILLAS E. 2015. Electrochemical mineralization of the antibiotic levofloxacin by electro-Fenton-pyrite process. Chemosphere 141: 250–257.

CHEN S, TANG L, FENG H, ZHOU Y, ZENG G, LU Y, YU J, REN X, PENG B, LIU X. 2019. Carbon felt cathodes for electro-Fenton process to remove tetracycline *via* synergistic adsorption and degradation. Sci Total Environ 670: 921–931.

CHEN Z, BI S, ZHAO G, CHEN Y, HU Y. 2020. Enhanced degradation of triclosan by cobalt manganese spinel-type oxide activated peroxymonosulfate oxidation process *via* sulfate radicals and singlet oxygen: mechanisms and intermediates identification. Sci Total Environ 711: 134715.

EL-GHENYMY A, RODRÍGUEZ RM, BRILLAS E, OTURAN N, OTURAN MA. 2014. Electro-Fenton degradation of the antibiotic sulfanilamide with Pt/carbon-felt and BDD/carbon-felt cells: kinetics, reaction intermediates, and toxicity assessment. Environ Sci Pollut Res 21(14): 8368–8378.

GANIYU SO, HUONG LE TX, BECHELANY M, ESPOSITO G, VAN HULLEBUSCH ED, OTURAN MA, CRETIN M. 2017. A hierarchical CoFe-layered double hydroxide modified carbon-felt cathode for heterogeneous electro-Fenton process. J Mater Chem A 5(7): 3655–3666.

GAO Y, WANG Y, ZHANG H. 2015. Removal of Rhodamine B with Fe-supported bentonite as heterogeneous photo-Fenton catalyst under visible irradiation. Appl Catal, B 178: 29–36.

Formatted: Highlight
Formatted: Highlight
Formatted: Highlight
Formatted: Highlight
Formatted: Highlight
Formatted: Highlight
Formatted: Highlight
Formatted: Highlight
Formatted: Highlight
Formatted: Highlight
Formatted: Highlight
Formatted: Highlight

*Corresponding Author: nguyentrungdung1980@gmail.com
nnhuy@hcmut.edu.vn

GAZI S, RAJAKUMAR A, SINGH NDP. 2010. Photodegradation of organic dyes in the presence of [Fe(III)-salen]Cl complex and H_2O_2 under visible light irradiation. J Hazard Mater 183(1): 894–901.

GUIVARCH E, TREVIN S, LAHITTE C, OTURAN MA. 2003. Degradation of azo dyes in water by electro-Fenton process. Environ Chem Lett 1(1): 38–44.

HAI H, XING X, LI S, XIA S, XIA J. 2020. Electrochemical oxidation of sulfamethoxazole in BDD anode system: Degradation kinetics, mechanisms and toxicity evaluation. Sci Total Environ 738: 139909.

HOU M-F, LIAO L, ZHANG W-D, TANG X-Y, WAN H-F, YIN G-C. 2011. Degradation of rhodamine B by Fe(0)-based Fenton process with H_2O_2. Chemosphere 83(9): 1279–1283.

HUONG LE TX, BECHELANY M, CRETIN M. 2017. Carbon felt based-electrodes for energy and environmental applications: a review. Carbon 122: 564–591.

LIN H, OTURAN N, WU J, ZHANG H, OTURAN MA. 2017. Cold incineration of sucralose in aqueous solution by electro-Fenton process. Sep Purif Technol 173: 218–225.

LIN H, ZHANG H, WANG X, WANG L, WU J. 2014. Electro-Fenton removal of Orange II in a divided cell: reaction mechanism, degradation pathway and toxicity evolution. Sep Purif Technol 122: 533–540.

MALEKI A, DARAEI H, HOSSEINI EA, AZIZI S, FAEZ E, GHARIBI F. 2015. Azo Dye DB71 Degradation Using Ultrasonic-Assisted Fenton Process: Modeling and Process Optimization. Arab J Sci Eng 40(2): 295–301.

Formatted: Highlight
Formatted: Highlight

*Corresponding Author: nguyentrungdung1980@gmail.com
nnhuy@hcmut.edu.vn

MI X, HAN J, SUN Y, LI Y, HU W, ZHAN S. 2019. Enhanced catalytic degradation by using RGO-Ce/WO_3 nanosheets modified CF as electro-Fenton cathode: influence factors, reaction mechanism and pathways. J Hazard Mater 367: 365–374.

NIDHEESH PV, GANDHIMATHI R. 2014a. Comparative Removal of Rhodamine B from Aqueous Solution by Electro-Fenton and Electro-Fenton-Like Processes. CLEAN-Soil Air Water 42(6): 779–784.

NIDHEESH PV, GANDHIMATHI R. 2014b. Removal of Rhodamine B from aqueous solution using graphite-graphite electro-Fenton system. Desalin Water Treat 52(10–12): 1872–1877.

NIDHEESH PV, GANDHIMATHI R, SANJINI NS. 2014. $NaHCO_3$ enhanced Rhodamine B removal from aqueous solution by graphite–graphite electro Fenton system. Sep Purif Technol 132: 568–576.

OANCEA P, MELTZER V. 2013. Photo-Fenton process for the degradation of Tartrazine (E102) in aqueous medium. J Taiwan Inst Chem E 44(6): 990–994.

OTURAN N, ARAVINDAKUMAR CT, OLVERA-VARGAS H, SUNIL PAUL MM, OTURAN MA. 2018. Electro-Fenton oxidation of para-aminosalicylic acid: degradation kinetics and mineralization pathway using Pt/carbon-felt and BDD/carbon-felt cells. Environ Sci Pollut Res 25(21): 20363–20373.

ÖZCAN A, ATILIR~~ATILIR~~ ÖZCAN A, DEMIRCI Y. 2016. Evaluation of mineralization kinetics and pathway of norfloxacin removal from water by electro-Fenton treatment. Chem Eng J 304: 518–526.

*Corresponding Author: nguyentrungdung1980@gmail.com
nnhuy@hcmut.edu.vn

Formatted: Highlight
Formatted: Highlight
Formatted: Highlight
Formatted: Highlight
Formatted: Highlight
Formatted: Highlight
Formatted: Highlight
Formatted: Highlight
Formatted: Highlight
Formatted: Highlight
Formatted: Highlight
Formatted: Highlight
Formatted: Highlight
Formatted: Highlight
Formatted: Highlight
Formatted: Highlight
Formatted: Highlight
Formatted: Highlight

PANG Y, RUAN Y, FENG Y, DIAO Z, SHIH K, HOU LA, CHEN D, KONG L. 2019. Ultrasound assisted zero valent iron corrosion for peroxymonosulfate activation for Rhodamine-B degradation. Chemosphere 228: 412–417.

PIMENTEL M, OTURAN N, DEZOTTI M, OTURAN MA. 2008. Phenol degradation by advanced electrochemical oxidation process electro-Fenton using a carbon felt cathode. Appl Catal, B 83(1): 140–149.

SAJA S, BOUAZIZI A, ACHIOU B, OUADDARI H, KARIM A, OUAMMOU M, AADDANE A, BENNAZHA J, ALAMI YOUNSSI S. 2020. Fabrication of low-cost ceramic ultrafiltration membrane made from bentonite clay and its application for soluble dyes removal. J Eur Ceram Soc 40(6): 2453–2462.

SENNAOUI A, ALAHIANE S, SAKR F, TAMIMI M, AIT ADDI EH, HAMDANI M, ASSABBANE A. 2019. Comparative degradation of benzoic acid and its hydroxylated derivatives by electro-Fenton technology using BDD/carbon-felt cells. J Environ Chem Eng 7(2): 103033.

SIRÉS I, GUIVARCH E, OTURAN N, OTURAN MA. 2008. Efficient removal of triphenylmethane dyes from aqueous medium by *in situ* electrogenerated Fenton's reagent at carbon-felt cathode. Chemosphere 72(4): 592–600.

SIRÉS I, OTURAN N, OTURAN MA, RODRÍGUEZ RM, GARRIDO JA, BRILLAS E. 2007. Electro-Fenton degradation of antimicrobials triclosan and triclocarban. Electrochim Acta 52(17): 5493–5503.

SUNDARAN SP, RESHMI CR, SAGITHA P, MANAF O, SUJITH A. 2019. Multifunctional graphene oxide loaded nanofibrous membrane for removal of dyes and coliform from water. J Environ Manage 240: 494–503.

*Corresponding Author: nguyentrungdung1980@gmail.com
nnhuy@hcmut.edu.vn

Formatted: Highlight
Formatted: Highlight
Formatted: Highlight
Formatted: Highlight
Formatted: Highlight
Formatted: Highlight
Formatted: Highlight
Formatted: Highlight
Formatted: Highlight
Formatted: Highlight
Formatted: Highlight
Formatted: Highlight
Formatted: Highlight
Formatted: Highlight

TENG X, LI J, WANG Z, WEI Z, CHEN C, DU K, ZHAO C, YANG G, LI Y. 2020. Performance and mechanism of methylene blue degradation by an electrochemical process. RSC Adv 10(41): 24712–24720.

TIAN J, OLAJUYIN AM, MU T, YANG M, XING J. 2016. Efficient degradation of rhodamine B using modified graphite felt gas diffusion electrode by electro-Fenton process. Environ Sci Pollut Res 23(12): 11574–11583.

TRAN MH, NGUYEN HC, LE TS, DANG VAD, CAO TH, LE CK, DANG T-D. 2019. Degradation of glyphosate herbicide by an electro-Fenton process using carbon felt cathode. Environ Technol 42(8): 1–10.

WU J, YANG J, HUANG G, XU C, LIN B. 2020. Hydrothermal carbonization synthesis of cassava slag biochar with excellent adsorption performance for Rhodamine B. J Cleaner Prod 251: 119717.

WU J, ZHANG H, OTURAN N, WANG Y, CHEN L, OTURAN MA. 2012. Application of response surface methodology to the removal of the antibiotic tetracycline by electrochemical process using carbon-felt cathode and DSA (Ti/RuO_2-IrO_2) anode. Chemosphere 87(6): 614–620.

XIAO W, GARBA ZN, SUN S, LAWAN I, WANG L, LIN M, YUAN Z. 2020. Preparation and evaluation of an effective activated carbon from white sugar for the adsorption of rhodamine B dye. J Cleaner Prod 253: 119989.

YANG J, SUN X, YANG W, ZHU M, SHI J. 2020. The Improvement of Coralline-Like $ZnGa_2O_4$ by Cocatalysts for the Photocatalytic Degradation of Rhodamine B. Catalysts 10(2).

Formatted: Highlight
Formatted: Highlight

*Corresponding Author: nguyentrungdung1980@gmail.com
nnhuy@hcmut.edu.vn

YU G, WANG Y, CAO H, ZHAO H, XIE Y. 2020. Reactive Oxygen Species and Catalytic Active Sites in Heterogeneous Catalytic Ozonation for Water Purification. Environ Sci Technol 54(10): 5931–5946.

YUAN S, FAN Y, ZHANG Y, TONG M, LIAO P. 2011. Pd-Catalytic *In Situ* Generation of H_2O_2 from H_2 and O_2 Produced by Water Electrolysis for the Efficient Electro-Fenton Degradation of Rhodamine B. Environ Sci Technol 45(19): 8514–8520.

ZAZOU H, OTURAN N, SÖNMEZ-ÇELEBI M, HAMDANI M, OTURAN MA. 2016. Mineralization of chlorobenzene in aqueous medium by anodic oxidation and electro-Fenton processes using Pt or BDD anode and carbon felt cathode. J Electroanal Chem 774: 22–30.

ZHANG J, ZHANG Z, ZHU W, MENG X. 2020a. Boosted photocatalytic degradation of Rhodamine B pollutants with Z-scheme CdS/AgBr-rGO nanocomposite. Appl Surf Sci 502: 144275.

ZHANG Y, LUO G, WANG Q, ZHANG Y, ZHOU M. 2020b. Kinetic study of the degradation of rhodamine B using a flow-through UV/electro-Fenton process with the presence of ethylenediaminetetraacetic acid. Chemosphere 240: 124929.

ZHU J, ZHU Z, ZHANG H, LU H, QIU Y. 2019. Calcined CoAl-layered double hydroxide as a heterogeneous catalyst for the degradation of acetaminophen and rhodamine B: activity, stability, and mechanism. Environ Sci Pollut Res 26(32): 33329–33340.

Formatted: Highlight
Formatted: Highlight
Formatted: Highlight
Formatted: Highlight
Formatted: Highlight
Formatted: Highlight
Formatted: Highlight
Formatted: Highlight
Formatted: Highlight
Formatted: Highlight
Formatted: Highlight
Formatted: Highlight

*Corresponding Author: nguyentrungdung1980@gmail.com
nnhuy@hcmut.edu.vn